

SEISMIC VULNERABILITY ASSESSMENT OF HISTORICAL MASONRY BUILDING UNDER NEAR-FIELD EARTHQUAKE

Ph.D. Thesis – Summary

For obtaining the scientific title of doctor at the

Polytechnic University of Timișoara

In the doctoral field of Civil Engineering and Installations

author Eng. Nicola CHIEFFO

Scientific coordinator Prof.habil.dr.eng. Marius Moșoarcă

July 2021

The Ph.D. thesis entitled “*Seismic vulnerability assessment of historical masonry building under near-field earthquake*” addresses the issue related to the seismic vulnerability concerning the historical buildings in non-reinforced masonry affected by the influence of the ground motion vertical component, bringing a refined calculation procedure with the aim of highlighting, on the one hand, the structural deficiencies of the existing buildings concerning near-field phenomena, on the other hand, proposes a methodology for mitigating the seismic risk.

Why this subject? Today, the increasing number of devastating seismic events have highlighted a reduced structural capacity of existing buildings towards seismic actions. In general, in the case of near-field seismic phenomena, it has been observed that the impulsive vertical excitation is one of the causes of the damage amplification, especially for existing unreinforced masonry construction typologies.

The prevailing aspect of the above-introduced seismic phenomena is to release all the seismic energy input in a very restricted urbanized area. In these circumstances, it is easy to understand how the effects induced on the existing building are seriously dangerous. The built heritage represents a historical testimony of a place and as such must be preserved. These issues are an important prerogative to sensitize the scientific community to an important aspect concerning the evaluation of the seismic vulnerability induced by the ground motion vertical component to not underestimate the possible induced effects.

What stands out in this thesis? The research was developed in five years, considering as a case study the Banloc Castle located in the homonymous Municipality of Banloc in the Banat Seismic Region. This URM building, severely damaged by the seismic sequence that occurred in 1991, showed multiple damages to the structural and non-structural elements. The numerical simulation was appropriately investigated by non-linear dynamic analysis to investigate the seismic performance of the examined building.

The analyses carried out are recognized and validated at the European level and propose a broad methodological approach for assessing the seismic vulnerability in the Banat Seismic Area, particularized for shallow earthquakes.

Another relevant aspect, the thesis provides valuable information about the failure mechanisms typical of the different types of historic buildings present in the epicentral area and opens up future research directions of great interest. The thesis is subdivided into 6 chapters, from general to particular, and presents 1 appendix. The chapters refer to an introduction of the proposed topic, to a presentation of the seismic assessment methodologies currently existing in the literature, the numerical simulation developed using a time-history procedure based on the real accelerograms of the seismic event Banat-Voiteg which occurred in 1991 focusing on two levels of detail, global and local analysis proposing a simplified procedure for the evaluation of

possible out-of-plane mechanisms in the case of the seismic vertical component. In the fifth chapter, the results obtained are extrapolated to derive the typological fragility and vulnerability curves for masonry buildings in the Banat area, following that at the end of the thesis presents the general conclusions, personal contributions, and future research guidelines.

In the first chapter, an introduction to the thesis is made. In particular, the proposed theme has been discussed providing an overview of the examined research topic and the current relevance of the investigated task creating parallelism with the near-field earthquakes that affected Central Italy [1]. The chosen area is the Municipality of Banloc characterized by a seismic history that significantly affected the URM structures erected in the epicentral area and the neighboring territories. The assessment of seismic vulnerability is formally carried out according to various approaches, based on specific procedures widely recognized at the European and worldwide levels [2-7]. However, most of the seismic codes [8-10] (Eurocode 8, NTC2018, Romanian Code P100-2019) are lacking to provide clear indications regarding the evaluation of the ground motion vertical component and provide design formulas only concerning the effects of horizontal acceleration ones. Furthermore, the methodologies proposed by the scientific literature are conservative for assessing the propensity to damage of the building heritage due to the influence of vertical seismic components, highlighting the necessity of an appropriate numerical calibration based on the damage detected after the past earthquakes.

As objectives, the thesis makes use of elaborating an accurate calculation procedure to take into account near-field phenomena providing important insights in this scientific domain. With this assumption, the effects of the impulsive earthquake have been evaluated considering the main engineering demand parameters, such as displacements and forces, focusing on two different scenarios, namely the horizontal and horizontal+vertical ground motions, deriving from the Banat-Voiteg earthquake that occurred in December 1991. These results have allowed defining the specific vulnerability and fragility curves for masonry buildings located in the epicentral area.

In the second chapter, a state-of-the-art considering the current existing methodologies has been discussed. Generally, the seismic risk indicates the probability of having an event (E) of a specific intensity of measurement (IMs) in a determined period (T) that causes a loss in a given area. Specifically, the seismic risk is conceived and quantified as a multifactorial combination of three random variables, such as hazard (H), exposure (E), and vulnerability (V) [11]. Regarding the vulnerability assessment, in the current state, the calculation procedures proposed in the literature can be classified as empirical, mechanical, or hybrid.

However, empirical methods evaluate the vulnerability of building aggregates based on the definition of typological classes: construction type; plano-altimetric distribution; the age of construction; functional aspects depending on the intended use. In particular, it is a semiotic approach according to which the level of detail of the analysis is adaptable to the degree and quality of the information available. Essentially, these methods allow establishing a uniqueness between the vulnerability index and damage caused by earthquakes. The quantification of the damage can be carried out through the definition of the typological vulnerability curves or, more commonly, through the damage probability matrices (DPM) for a determined class of vulnerability, based on the statistical processing of the damages caused by events that occurred (a posteriori analysis). The empirical procedures are based on an observational assessment of the vulnerability induced by a hypothetical reference seismic scenario [12-15]. These procedures do not require a wide level of information, however, they require an appropriate typological classification to implement a rapid preliminary study at the urban level. Among the empirical methodologies, the most used is the "probable damage matrix", the "vulnerability

index method" [16], [17], respectively the "continuous vulnerability curves method" [18], [19].

Mechanical methods are more sophisticated procedures than the previous ones as they require a level of detail such as to be able to perform numerical simulations using a mechanical-analytical approach. In this circumstance, non-linear analyses are performed to evaluate the seismic response of a given structure. The associated damage can be assessed by reaching a limit state identifiable by the achievement of a limit tensional state or a collapse mechanism of the structure. Among the best known, we note the "method of analytically derived vulnerability curves" [20] used in the RISK-EU research project [21], "method based on yield mechanisms" [8], respectively "method based on spectrum capacity" [22] widely used in the HAZUS or HAZARD US research project [23].

Finally, hybrid methods are derived from the combination of previously defined methods. This macroseismic approach is based on the definition of the European Macroseismic Scale EMS-98 [24], which implicitly defines a model of vulnerability and is applicable also in the European context.

However, all the methodologies presented essentially aim at an assessment of the seismic vulnerability taking into consideration only and exclusively the effects caused by the horizontal seismic action, implicitly neglecting the effects induced by the ground motion vertical component.

Chapter three in the first phase of the activity framework has been highlighted the aspects concerning the seismicity of the Banat Seismic Region. In general, the Romanian tectonic system is made up of pre-Alpine orogenic units (i.e. deriving from an orogenic process, in which the predominant reliefs consist of rocky masses that have undergone a tectonic deformation due to lateral thrust) characterized by the presence of Moldavian plates, from the Eastern Carpathians (Apuseni Mountains) and in the Eastern sector from the Transylvanian depression. The complex tectonic system has generated important crustal earthquakes due to the presence of faults identified along the contact lines of the tectonic plates themselves. Thus, in Fig. 1, the tectonic structural systems (Fig. 1(a)) and the distribution of the epicenters associated with the fault mechanisms (Fig. 1(b)) that occurred have been presented [25].

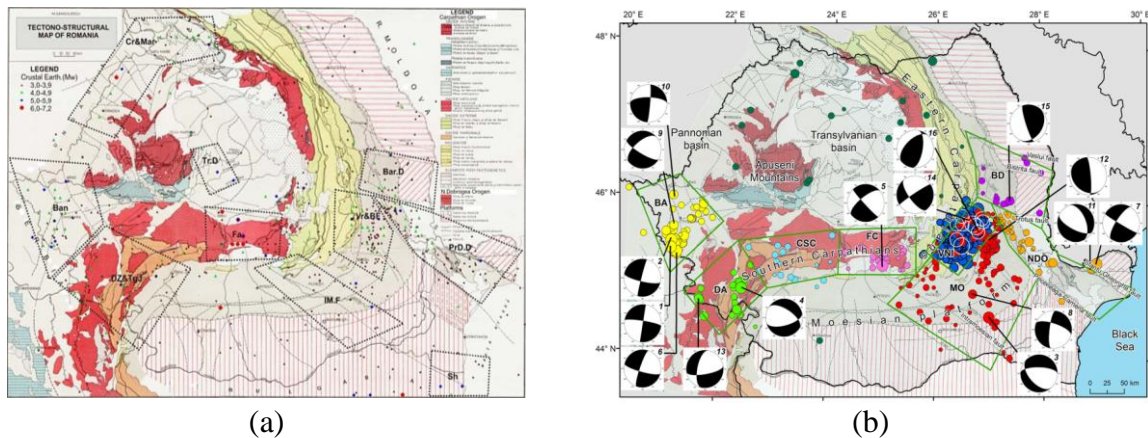


Figure 1: Romanian's tectonic plates (a) and fault mechanisms (b)[25].

Focusing on the Banat region, assumed as a study area, it consists of a dense capillary network of faults. The hypocenters in the Banat area have been estimated at 5 km and 33 km [145]. Recently, the earthquake catalog concerning the entire Banat area was updated, using a complete set of condensed and processed data regarding geology, geophysics. In particular, three zones with different seismicity have been defined, i.e. Sinnicolau Mare-Arad, Timisoara and Banloc-Voiteg, Oravita, based on the distribution of the earthquakes that occurred with a

moment magnitude $M_w > 5.3$ in a period between 1990 and 1995 (Fig. 2) [26].

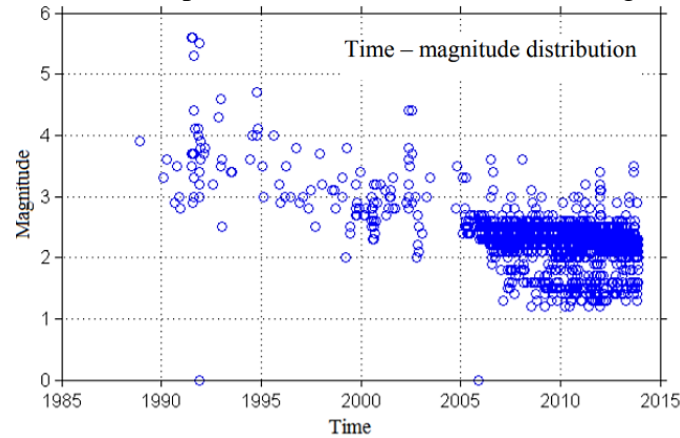


Figure 2: Earthquakes occurred in Banloc between 1988 and 2015 [26].

In the second phase, the Banloc Castle has been introduced considering its architectural and functional aspects and its state of conservation. In general, the case study building is the most important monument of the municipality and it has been completed in 1759. It is located in the center of the homonymous city of Banloc and it is a massive building with a "U" shape plan built at the beginning of the 19th century. Structurally, the castle is an imposing building with very thick and heavy solid brick walls with maximum plan dimensions are 38.80 m x 24.20 m. It is consisting of a ground floor, intermediate floor, and massive wooden roof. They have a thickness of 1.30 m on the ground floor, the external walls on the first floor, made of the same material, are 0.90 m thick while the internal walls have a thickness of 0.80 m. On the upper part, there are vaulted ceilings with a thickness of 0.25 m. The roof is solid and robust, with a wooden supporting structure whose construction technique was used in the Banat region. The heights between the floors are 4.0 m and 5.70 m, respectively [27].

Concerning the post-earthquake damage assessment, the Banloc earthquake that occurred on 07-12-1991 at a focal depth of 9 Km was considered as a reference seismic scenario. The seismic energy released produced a magnitude (M_w) of 5.5 according to the Richter scale. Considering the reduced focal depth, this event is best classified as a medium-depth geological event. Moreover, it is characterized by a reduced site-source distance (7.01 km far from the epicenter), which makes it a near-field event. The earthquake intensity (epicentral intensity) associated with the event that occurred was VII-VIII according to Mercalli Intensity Scale (MCS) as reported in Fig. 3 [28].

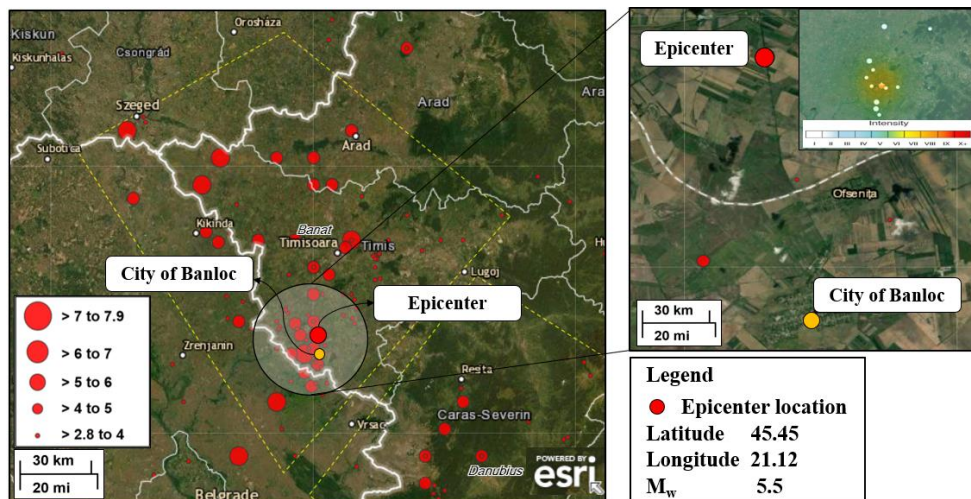


Figure 3: Geographical identification of the event that occurred in Banloc on 07-12-1991

[28].

The achieved post-earthquake damages were introduced and discussed. Being a near-field event, the seismic vertical component produces a consistent level of damage, especially in the horizontal structures and, subsequently, with the arrival of the horizontal components, the damage extends to vertical structures mainly in the spandrel beams due to the formation of shear failures as reported in Fig. 4 [29].

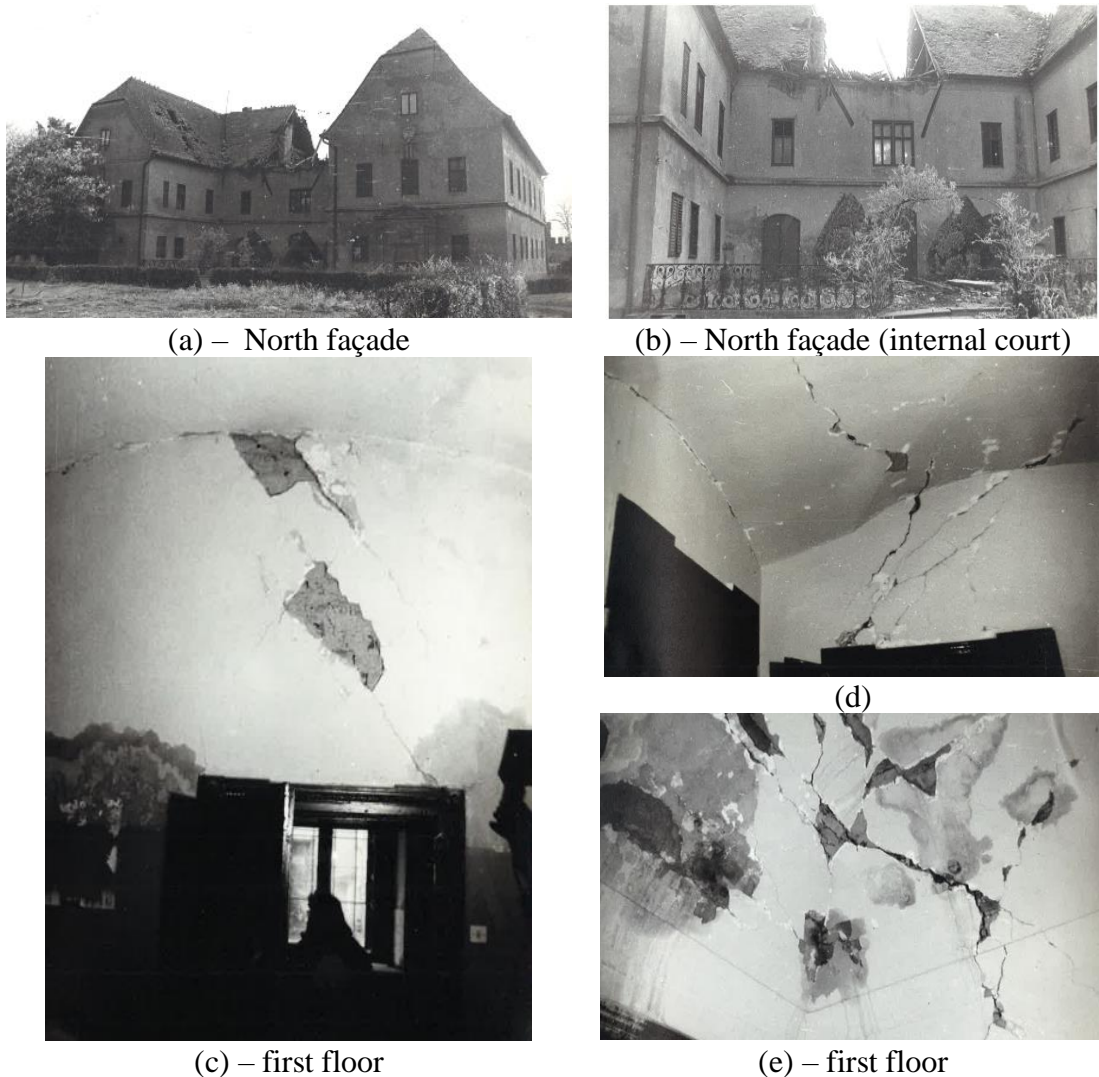


Figure 4: Detected damages on the Banloc Castle after the 1991 earthquake [29].

Regarding the aspects related to numerical simulation, the building model was implemented by adopting the finite element software DIANA FEA [30]. The software is also equipped with powerful solvers to optimize the solution procedures for all types of complex linear and nonlinear models with accurate results and quick and reliable calculations. FEM is a refined computational numerical technique most commonly used to solve complex engineering problems. The analysis of historic masonry buildings represents a very complex task that depends on numerous factors that can significantly influence the expected output. In general terms, this problem can be addressed by considering two main aspects, such as (i) simplification of the geometric model and (ii) idealization of materials. Based on these assumptions, the FEM model of the Banloc Castle is presented in Fig. 5. In particular, the case study geometric model consists of a set of shell elements suitably interconnected with 255000 nodes, appropriately

named DOF, the acronym for a degree of freedom.

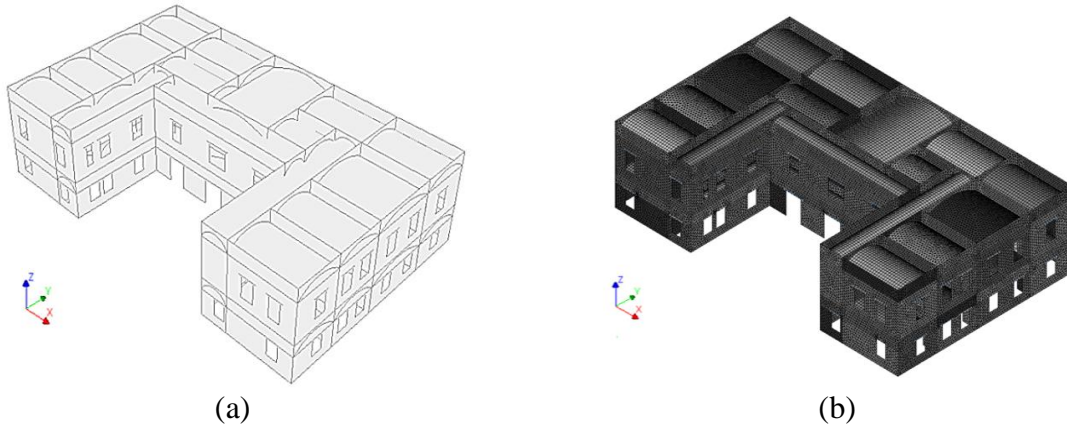


Figure 5: FEM model of the Banloc Castle, (a) 3D model, and (b) global shell elements.

About the material properties, the Romanian historical heritage has similar construction and material characteristics of the buildings located in the Northern part of Italy and for this reason, the mechanical characteristics of the masonry were adopted about the experimental data used by the Italian Code [10] as reported in Table 1.

Table 1. Mechanical properties of the masonry [10].

Mechanical Properties		
Modulus of elasticity	E [N/mm ²]	1500
Shear modulus	G [N/mm ²]	500
Compressive strength	f_m [N/mm ²]	2.40
Tensile strength	f_t [N/mm ²]	0.24
Tangential strength	τ_o [N/mm ²]	0.06
Specific weight	w [KN/m ³]	18
Poisson ratio	ν [-]	0.20
Fracture energy (compression)	G_{fc} [N/mm]	4.64
Fracture energy – Mode I (tensile)	G_{ft} [N/mm]	0.012

Subsequently, a non-linear dynamic analysis has been performed considering the real accelerograms of the Banat-Voiteg earthquake that occurred in 1991. The seismic loads are characterized by maximum peak amplitude in X direction (Longitudinal) of 0.80 ms^{-2} , in Y direction (Transversal) of 1.30 ms^{-2} , and Vertical direction of 1.30 ms^{-2} . Considering the time domain, a time history of 10 seconds has been plotted since all the energy content has been released [31]. Furthermore, to characterize the influence of the vertical component, the ratio between vertical spectral acceleration, V, and the corresponding horizontal spectral ones, H, are shown below. In particular, the V/H PGA spectral ratios in the two directions X and Y, are plotted. Thus, for NF phenomena, the V/H PGA ratio is generally greater than 1 exceeding the 2/3 limit imposed by Newmark and Hall [32] (Fig. 6).

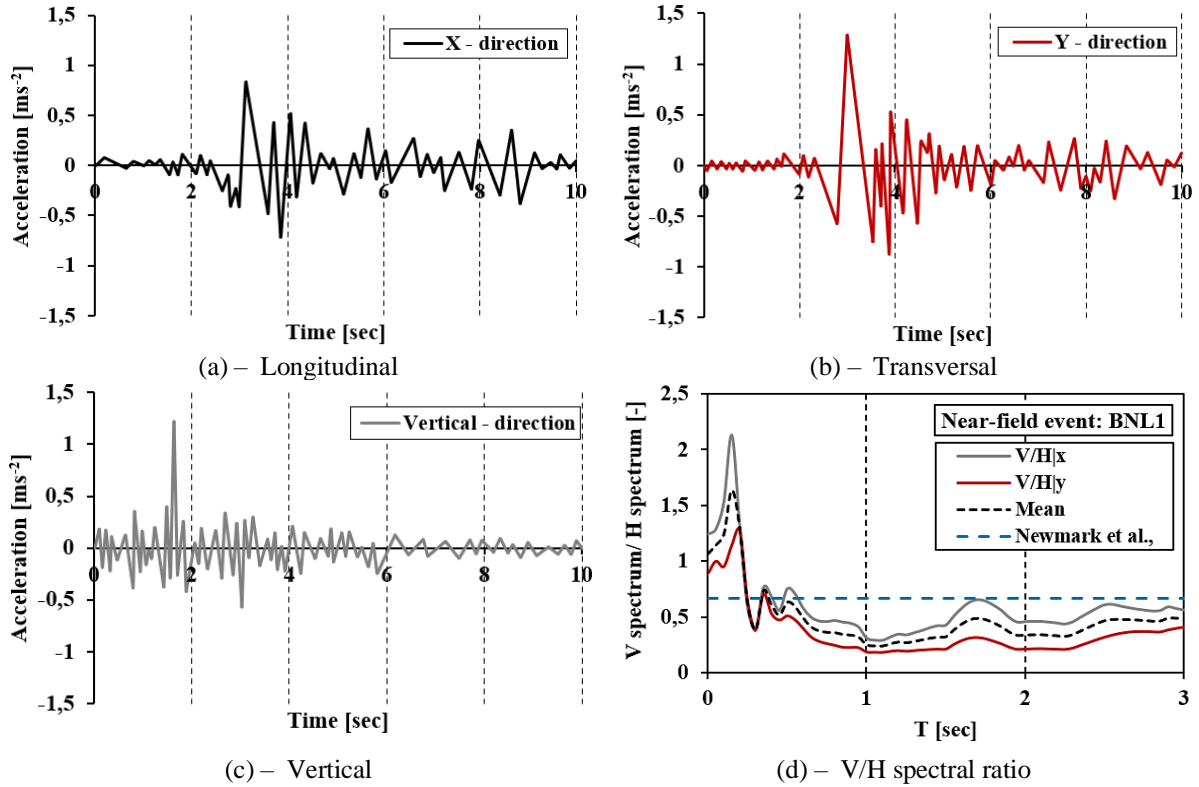


Figure 6: Seismic load evaluated in all dynamic directions (a-c) and (d) Vertical to horizontal spectral ratio.

Chapter four presented the results obtained from the numerical simulation. In particular, the analysis results take into consideration two aspects concerning the global and local capacity of the investigated structure. In the first analysis phase, a global behavior has been analysed by considering two distinct scenarios named (H+V) and (H), respectively, to simulate the seismic effects in which the vertical component of ground motion has been considered (scenario H+V) and neglected (scenario H).

To this purpose, specific comparisons have been done providing interesting insights considering the following variable parameters: (i) energy dissipation capacity; (ii) stiffness degradation; (iii) ductility displacements, and (iv) behavior factor, q , which was suitably compared with the provisions of the EC8 and Romanian Code [8], [9].

First of all, the analysis of the Engineering Demand Parameters, EDPs, was conducted considering above mentioned scenarios to better highlight the influence of the vertical ground motion (VGM) as summarized in Fig. 7 [33-37]. Particularizing the results obtained it was noticed how the seismic demand in the vertical direction has produced a significant increase in terms of axial forces regime when it is compared to the case in which it was neglected (scenario (H)) as reported in Fig. 7 (a). Moreover, there was no variation of the base shear between the two scenarios (H) and (H+V), respectively (see Fig. 7 (b-c)). Consequently, in Fig. 7 (d) it was possible to note that globally for the entire time history, the average variation in terms of axial force regime between the two scenarios considered was around 100%. In particular, at $t=1.68$ sec, which corresponds to the vertical acceleration peak, the axial force's variation for the scenario (H+V) was higher than the corresponding scenario (H) [33].

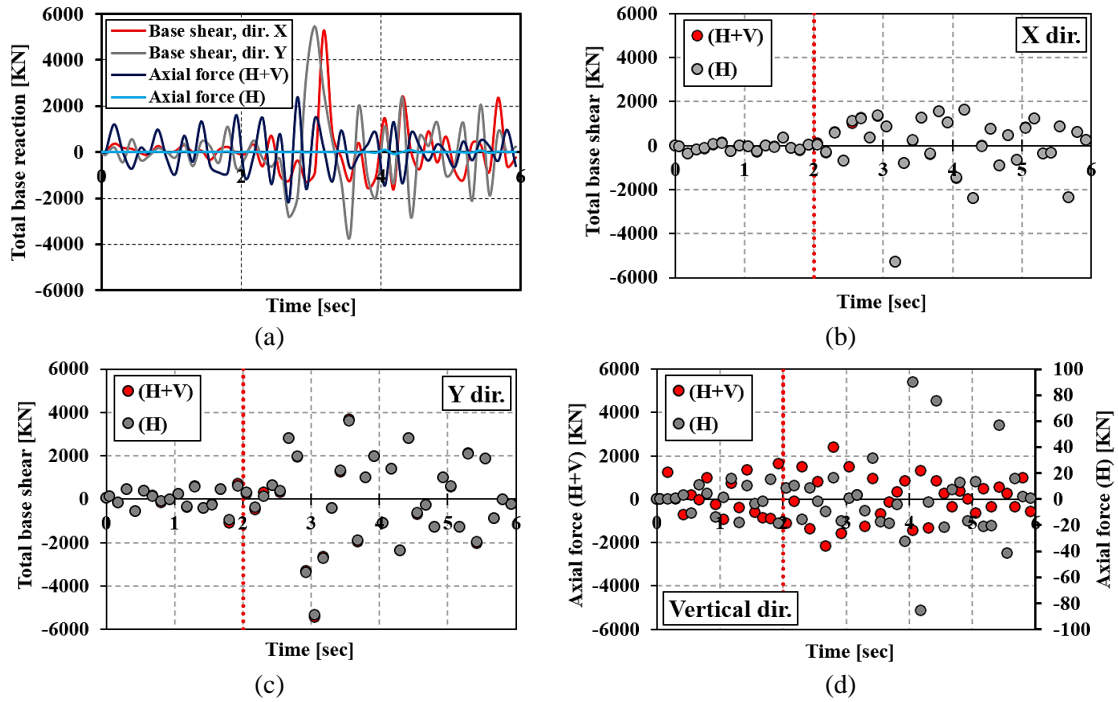


Figure 7: Time histories of total base reaction for the two analysed scenarios, (H) and (H+V), respectively.

Subsequently, the effects of the vertical seismic component were analysed in terms of displacements. Therefore, 38 monitoring points have been selected, that is 19 for each floor. For a clearer and more accurate overview, Fig.8 shows the MP relating to the second level, specifying that the respective control nodes at the first level are placed on the same alignment.

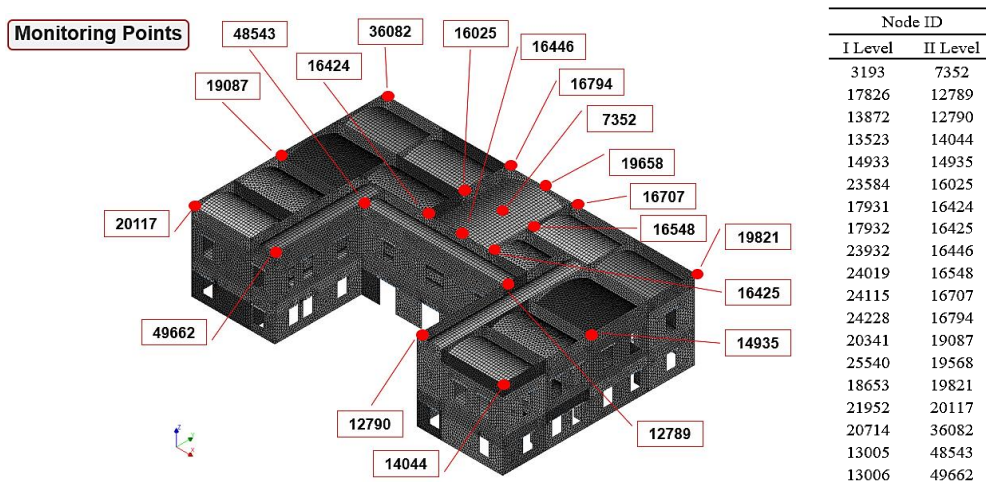


Figure 8: Selected monitoring point (MP) for the case study building.

Furthermore, Table 2 has shown the absolute displacements afferent to all the MPs located on the second floor of the building diversifying the position of the point placed on the vault, V, from those afferent on the wall panels, WP.

Table 2. Displacements time history of the selected MPs.

Position	MP	Displ. (H+V) [cm]			Displ. (H) [cm]			Δ_x [%]	Δ_y [%]	$\Delta_{vert.}$ [%]
		X	Y	Vert.	X	Y	Vert.			
V	7352	2.74	3.93	0.77	1.74	0.73	0.08	57	438	863
WP	12789	1.79	0.82	0.33	1.74	0.80	0.18	3	2	83
WP	12790	2.31	0.32	0.02	2.31	0.29	0.02	-	10	-
WP	14044	2.31	1.24	0.11	2.29	1.17	0.08	1	6	38
WP	14935	3.24	0.85	0.04	3.12	0.80	0.03	4	6	33
WP	16025	1.78	1.21	0.03	1.75	1.17	0.00	2	3	-
WP	16424	1.73	1.16	0.04	1.71	1.10	0.02	1	5	100
WP	16425	1.71	1.46	0.06	1.68	1.43	0.04	2	2	50
WP	16446	1.58	1.40	0.05	1.57	1.30	0.02	1	8	150
WP	16548	1.86	1.51	0.06	1.87	1.41	0.03	1	7	100
WP	16707	1.11	0.64	0.08	1.12	0.58	0.05	1	10	60
WP	16794	1.16	0.45	0.06	1.16	0.44	0.02	-	2	200
WP	19087	3.22	0.68	0.04	3.14	0.61	0.01	3	11	300
WP	19568	1.08	1.12	0.06	1.08	1.04	0.03	-	8	100
WP	19821	1.26	0.55	0.12	1.22	0.50	0.05	3	10	140
WP	20117	2.65	0.51	0.12	2.60	0.43	0.05	2	19	140
WP	36082	1.43	0.84	0.12	1.31	0.78	0.06	9	8	100
WP	48543	1.43	1.42	0.05	1.43	1.34	0.04	-	6	25
WP	49962	2.78	1.64	0.04	2.74	1.57	0.08	1	4	50

By comparing the two analysed scenarios (H) and (H+V) it was shown how the seismic vertical component has produced an average percentage displacements increase enclosed in the range [5%-133%] concerning the case in which the vertical component was neglected. Moreover, the ground motion vertical component has increased the displacements of the building in Y direction more than in X direction, since, given the asymmetry, was subject to torsional phenomena. Considering the MP placed on the vault (MP 7352) was subject to a higher influence of the ground motion vertical component with a considerable displacement increase ($\Delta_{vert.} >> 100\%$) compared to the scenario (H) and finally, the control nodes located in the corner positions were much more sensitive to the effects of VGM which influence the seismic demand [33], [37].

Subsequently, the evaluation of the displacement ductility afferent to the case study building was analyzed. In such circumstances to characterize the dynamic behavior of the case study building, the above-presented monitoring points were considered to idealize the structural behavior as an equivalent elastic-plastic system and for each of them, the non-linear cyclic behavior was enveloped, as proposed by [38]. Moreover, Tables 3 and 4 have reported the results in terms of the maximum force (F_{max}), yield displacement (d_y), ultimate displacement (d_u), and the evaluated ductility factor, μ , in positive and negative directions, diversifying the point located on the vault, V, from those afferent on the wall panels, WP, respectively.

Table 3. Main capacity parameters in X analysis direction.

X-direction									
Pos.	Node ID	Positive direction (X ⁺)			μ^+ factor	Negative direction (X ⁻)			μ^- factor
		d _y [cm]	d _u [cm]	F _{max} [KN]		d _y [cm]	d _u [cm]	F _{max} [KN]	
V	7352	0.37	1.46	2401.71	2.95	-0.31	-1.37	1622.06	3.35
WP	12789	0.25	1.33	2362.21	4.32	-0.25	-1.86	1622.10	6.44
WP	12790	0.65	2.65	2501.71	3.05	-0.50	-1.63	1622.06	2.26
WP	14044	0.18	0.96	2401.71	4.30	-0.22	-1.27	1622.06	4.80
WP	14935	0.25	0.64	2362.21	1.56	-0.20	-1.20	1264.49	5.00
WP	16025	0.15	1.32	2401.71	7.83	-0.10	-0.66	1622.06	5.55
WP	16424	0.20	1.14	2362.21	4.70	-0.20	-0.69	1622.06	2.45
WP	16425	0.10	0.87	2401.71	7.70	-0.10	-0.60	1622.00	5.00
WP	16446	0.15	1.01	2362.00	5.73	-0.15	-0.60	1622.00	3.00
WP	16548	0.20	1.01	2401.71	4.05	-0.20	-1.00	1622.00	4.00
WP	16707	0.20	1.01	2401.71	4.05	-0.20	-0.61	1622.00	2.07
WP	16794	0.20	1.01	2401.71	4.05	-0.20	-0.61	1622.00	2.07
WP	19087	0.40	2.15	2501.71	4.38	-0.20	-1.20	1646.94	5.00
WP	19568	0.15	0.87	2401.00	4.80	-0.15	-0.50	1646.94	2.33
WP	19821	0.15	1.24	2401.71	7.30	-0.15	-0.85	1622.06	4.65
WP	20117	0.22	1.83	2401.71	7.32	-0.15	-0.40	1700.00	1.67
WP	36082	0.11	0.62	2462.00	4.64	-0.10	-0.57	1622.00	4.66
WP	48543	0.30	1.56	2501.00	4.20	-0.25	-1.66	1622.06	5.64
WP	49662	0.20	1.55	2362.00	6.75	-0.15	-1.20	1622.06	7.00
Minimum		0.10	0.62	2362.00	1.56	-0.10	-0.50	1264.49	2.07

Table 4. Main capacity parameters in X analysis direction.

Y-direction									
Pos.	Node ID	Positive direction (Y ⁺)			μ^+ factor	Negative direction (Y ⁻)			μ^- factor
		d _y [cm]	d _u [cm]	F _{max} [KN]		d _y [cm]	d _u [cm]	F _{max} [KN]	
V	7352	1.35	3.93	5456.92	1.68	-1.07	-2.62	3659.85	1.39
WP	12789	0.23	1.78	3316.64	3.53	-0.17	-1.11	3659.85	3.17
WP	12790	0.30	2.25	3316.64	3.46	-0.25	-1.87	3659.85	3.46
WP	14044	0.30	1.97	3316.64	3.18	-0.20	-1.22	3765.85	3.04
WP	14935	0.20	1.70	3316.63	7.48	-0.20	-1.41	3765.85	6.05
WP	16025	0.30	2.40	3316.00	7.00	-0.30	-1.59	3700.00	4.30
WP	16424	0.50	3.52	3416.64	6.03	-0.50	-2.77	3750.00	4.54
WP	16425	0.40	3.09	3416.64	6.73	-0.40	-2.34	3800.00	4.86
WP	16446	0.30	2.09	3416.64	5.97	-0.30	-2.34	3800.00	6.80
WP	16548	0.30	2.39	3416.64	6.97	-0.30	-1.62	3659.85	4.40
WP	16707	0.60	3.77	3416.64	5.28	-0.60	-3.28	3800.00	4.47
WP	16794	0.50	2.83	3416.64	4.66	-0.40	-3.28	3800.00	7.20
WP	19087	0.22	1.57	5556.92	6.15	-0.20	-1.91	3759.00	8.53
WP	19568	1.63	5.39	3316.00	2.31	-1.20	-5.22	3900.00	3.35
WP	19821	0.30	1.83	3466.00	5.11	-0.40	-1.49	3659.85	2.73
WP	20117	0.20	1.77	3416.64	7.84	-0.30	-2.40	3600.00	7.00
WP	36082	0.60	1.72	3416.64	1.87	-0.70	-2.02	3600.00	1.89
WP	48543	0.20	1.72	3316.00	7.61	-0.25	-2.24	3700.00	7.96
WP	49662	0.25	2.13	3316.00	7.52	-0.28	-2.45	3650.00	7.75
Minimum		0.10	1.57	3316.00	1.68	-0.17	-1.11	3600.00	1.39

The maximum shear threshold in Y direction ($F_{Ymax} = 3600$ KN) is 34% higher than the corresponding threshold in the orthogonal direction ($F_{Xmax} = 2362$ KN).

In X direction the structure has resented a geometric asymmetry resulting affected by torsional phenomena, thus, the yielding and ultimate displacements are 55% and 52% lower than those estimated in Y direction. The minimum ductility factor estimated for the horizontal structures in the two analysis directions, X and Y, was equal to 1.39. By comparing the global behavior in terms of ductility for the vertical structures, it has been observed that in Y direction, the minimum ductility ($\mu_{Ymin} = 1.89$) was 17% higher than that in the orthogonal direction, $\mu_{Xmin} = 1.56$.

The analysis of the stiffness degradation is an important step to take into consideration since it provides indications regarding the safety level (local or global) of the structural system and the corresponding energy dissipation.

In this perspective, the stiffness degradation was calculated using Equation 1 [38]:

$$K_i = \frac{|+F_{max,i}| - |-F_{max,i}|}{|+\Delta_{max,i}| - |-\Delta_{max,i}|} \quad (1)$$

where $F_{max,i}$ is the absolute value of the positive and negative peak lateral forces of the i -th cycle and $\Delta_{max,i}$ represents the corresponding absolute value of the positive and negative displacements associated with the i -th cycle. The results have shown in Fig. 9

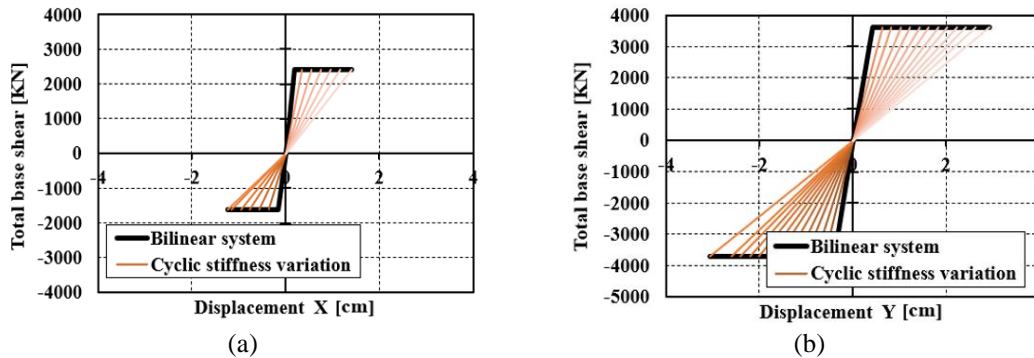


Figure 9: Cyclic stiffness degradation in, (a) X direction and (b) Y direction.

From the results acquired, the main aspects underline in terms of stiffness degradation, it has been shown how in X direction the initial secant stiffness, K_0 , is greater than 70% concerning the secant stiffness offered in the perpendicular direction, Y. The stiffness degradation evaluated in Y direction was 67% higher than that in the orthogonal direction.

So, to better understand the response of the building, the behavior factor was determined considering two different approaches, force [39] and energetic [40], [41] concerning the ductility previously determined. In particular, three distinct cases were analysed, by considering (i) maximum vertical decompression peak, estimated at 2 sec, which corresponds to 33% of the energy dissipation; (ii) maximum compression due to vertical seismic motion, estimated at 3 sec, which corresponds to 50% of the structural capacity; (iii) the entire time-history, $t=6$ sec, i.e. 100% of the hysteretic dissipation. This choice was supported by investigating the influence of the ground motion vertical component on the expected behavior factor, q .

For an exhaustive overview, Fig. 10 graphically shows the summary of the results above introduced in which the variation of the expected ductility is correlated to the behavior factor, for the capacity threshold evaluated at 33% of the energy dissipation.

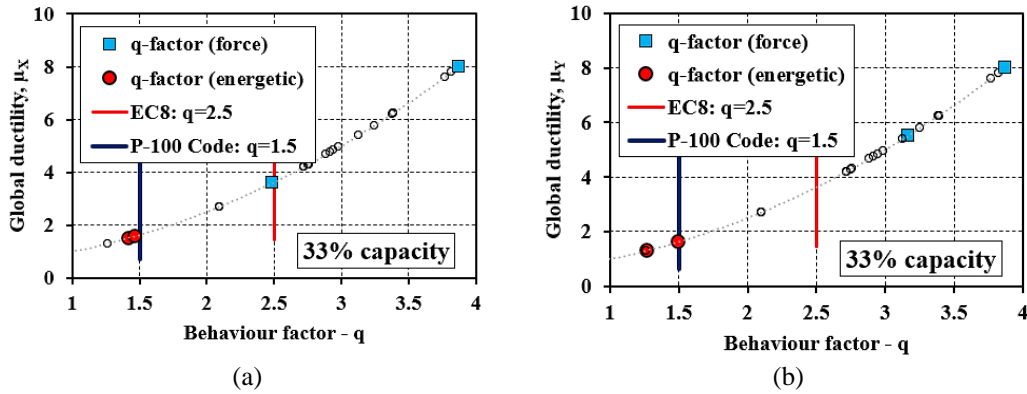


Figure 10: Ductility-q factor law for capacity variation of 67%.

In general, it was observed that by comparing the values of the behavior factor, q , obtained using the force approach for energy dissipation of 67% ($q = 2.48$) and 50% ($q = 2.53$), was very close to the prescription of EC8 [8] while by considering the energetic approach, the estimated behavior factor, q , was contained in the range [1.18-1.46] resulting in complies with the limit of 1.50 imposed by the Romanian Design Code P-100 [9].

Regarding the local analysis, the time-history axial load variation has been analysed to consider the influence of the ground motion vertical component (Fig. 11). In this condition, the previous scenario, (H) and (H+V) have been considered normalizing the axial load with respect to the corresponding value offered by gravitational loads, N_{grav} [33].

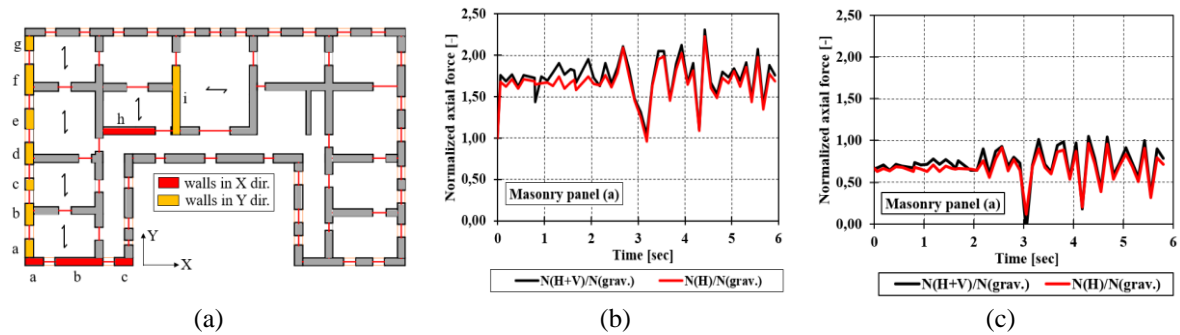


Figure 11: Normalized axial force in case of impulsive earthquake for the masonry walls in X (a) and Y (b) directions.

It has been observed that in X direction, in the first two seconds of the time domain, the vertical component affects the behavior of the wall panel by approximately 12% more than the scenario (H). In Y direction, this difference is around 8%. Furthermore, for $t > 2$ sec. in both analysis directions, there is a minimal difference between the two scenarios of 4% since the vertical component loses its energy input.

Furthermore, the shear capacity of the wall panels was considered through the study proposed by Cacovic et al, [42]. In addition, rocking- behavior was also analysed. Following the EC8 [8], the minimum shear threshold reached in the masonry panel represents the first activated mechanism. Based on these conditions, the results are shown in Fig. 12 highlighting the masonry panels most sensitive to the influence of the ground motion vertical component.

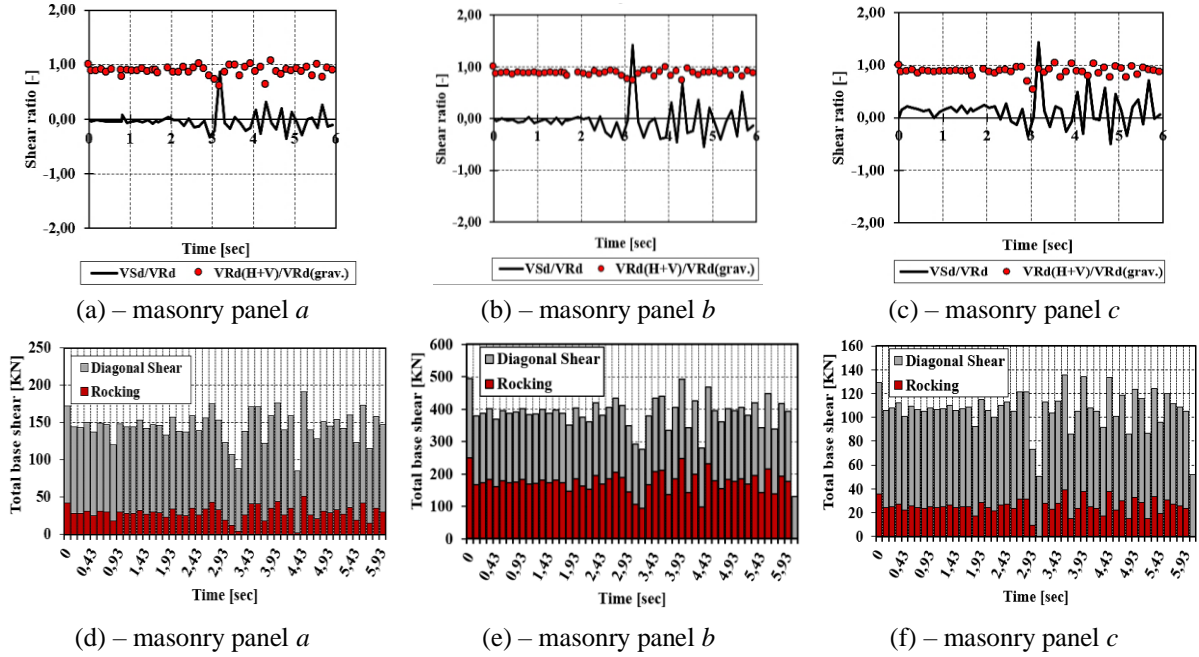


Figure 12: Shear force verifications (a-c) and rocking mechanisms (d-f) for the masonry panel oriented in X direction.

The results show that the vertical seismic acceleration in the first two seconds of the time domain does not induce diagonal shear cracks. However, for $t > 2$ sec, with the arrival of the horizontal components, it is noted that the shear verification was not satisfied. This circumstance demonstrates how the ground motion vertical component reduces both, the bearing capacity of the masonry, and the corresponding shear resistance, respectively (Fig. 12 (a-c)). Furthermore, it was observed that the rocking mechanism was activated first concerning diagonal failure with a minimum shear threshold approximately 2 times lower than the corresponding values associated with the diagonal shear (Fig. 12 (d-f)).

Subsequently, the strength domains are a useful tool to validate the possible failure mechanisms that could occur in a wall system when subjected to seismic action. As a result of these seismic actions, it is possible to use the flexural and shear resistance domains to define the strength capacity of each masonry wall according to the study proposed by Augenti (2009) [43].

In particular, the strength domains are characterized by specific rupture boundaries that identify the main failure mechanisms. Moreover, there are different failure thresholds to consider: (i) non-cracked elastic condition; (ii) cracked elastic condition; (iii) plastic condition due to bending and the interaction with the failure mechanisms induced by shear. Methodologically, by fixing the maximum axial threshold, it was possible to determine the intersection with each boundary condition to estimate the maximum shear threshold that activates the failure mechanism in the masonry panels. Consequently, the capacity curves of the masonry panel were defined based on the elastic, post-elastic, and ultimate displacements derived according to [43] and reported in Equations 2-4. Thus, the results have been depicted in Fig. 13 for the masonry panel b oriented in X direction.

$$\delta = \delta_v + \delta_m = \chi \cdot \frac{V \cdot H}{G \cdot A} + \frac{V \cdot H^3}{12 \cdot E \cdot I} \quad \text{elastic displacement} \quad (2)$$

$$\delta_f = 1.2 \cdot \delta \quad \text{post-elastic displacement} \quad (3)$$

$$\delta_u = 1.5 \cdot \delta \quad \text{ultimate displacement} \quad (4)$$

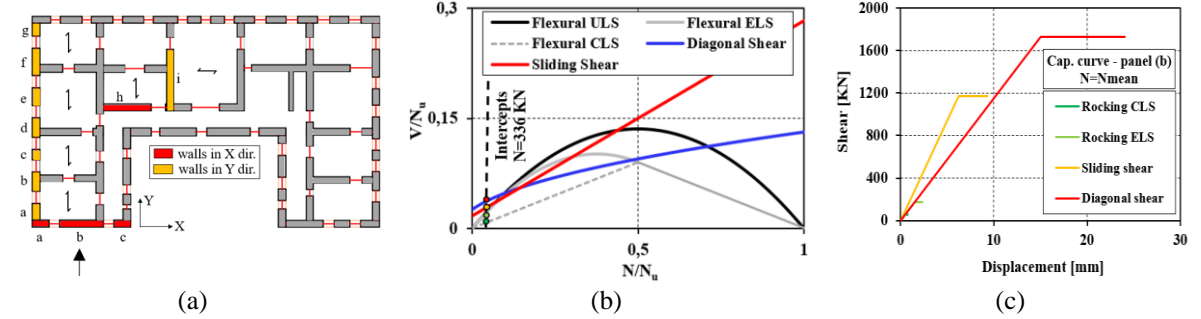


Figure 13: Strength domain and capacity curves for the masonry panel b oriented in X direction.

In general, it was observed that for each wall panel examined, the mechanisms in the elastic phase (rocking) are activated for very low shear threshold values, while the shear mechanisms (diagonal and sliding) are activated for high shear values which correspond to axial stress variations of 1.8% and 2.7% of the ultimate capacity of the panel, N_u .

In the third analysis, the out-of-plane mechanisms have been evaluated in the case of near-field seismic phenomena. The question to ask is, *how does the vertical seismic force need to be considered in the evaluation of the collapse mechanisms?* The study proposed by [44] has shown how the effect of the vertical seismic force creates a system of vertical inertial forces that contribute to the activation of the collapse mechanism. This vertical inertial action progressively tends to create a system of overpressures and decompressions that cyclically degrade the mechanical characteristics of the masonry material [45].

Therefore, based on these considerations, the proposed procedure aims to analyse the possible out-of-plane mechanisms in the case of shallow earthquakes characterized by high horizontal actions and lower vertical acceleration. Specifically, the maximum vertical seismic component in compression was evaluated at the time step in which the horizontal seismic actions act simultaneously, neglecting the ground vertical component in the decompression phase since the lack of friction and cohesion between the mortar and brick elements subsisted.

The North façade was analysed since it was characterized by out-of-plane mechanisms (given by the bending overturning) after the Banat-Voiteg earthquake. Thus, the possible collapse mechanisms were suitably analysed using 3Muri software [46]. The software, starting from the definition of the basic geometry, automatically identifies the possible mechanisms that could be activated based on the mechanical characteristics of the masonry, constraint, and load conditions. The results have been summarized in Fig. 14.

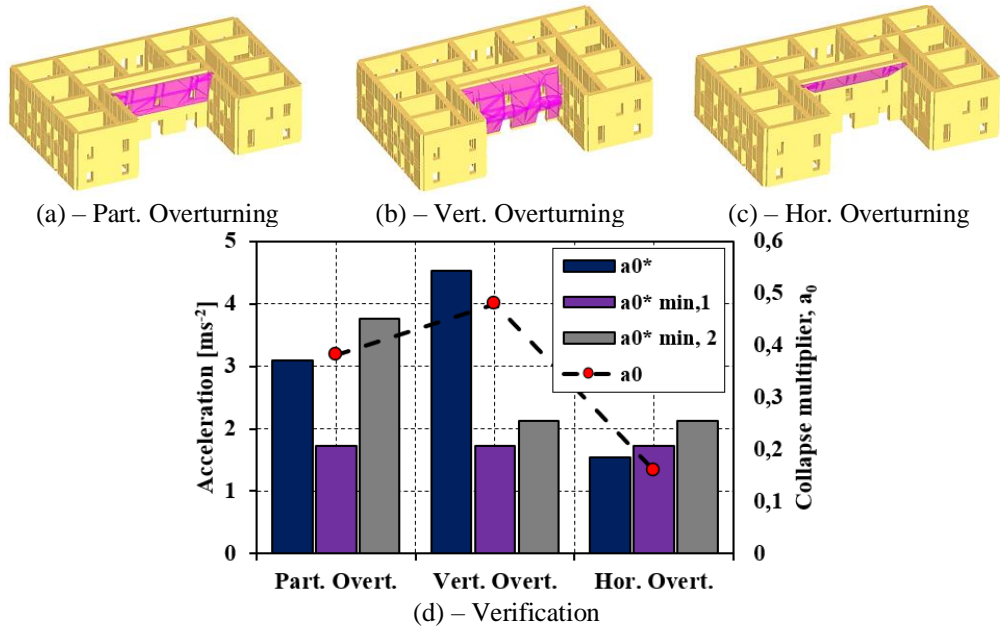
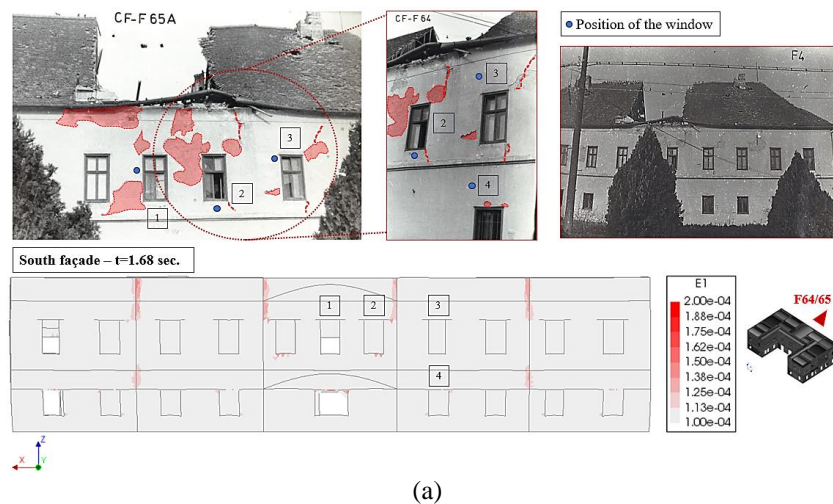


Figure 14: Multiplier factor, a_0 , Vs mechanisms considering the compressive effects of VGM for the North façade.

Finally, the numerical damage has been compared to the real ones that occurred in the epicenter. It was observed that the vertical earthquake induces a state of overpressure and decompression that cyclically affects the resistance of the material, which, exceeding the tensile strength, tends to damage. The cracks activated represent a condition of energy dissipation of the structure to the detriment of its static integrity. Once again, the ground motion vertical component locally modifies the mean shear stress (horizontal and vertical) since it intrinsically alters the compression stress regime according to [43]. In fact, during the time history cycle, the vertical component of the seismic action changes its sign, causing a continuous variation of the axial compression stress which also governs the shear resistance.

A representation of the damage calibration between simulated and real ones is shown in Fig. 15.



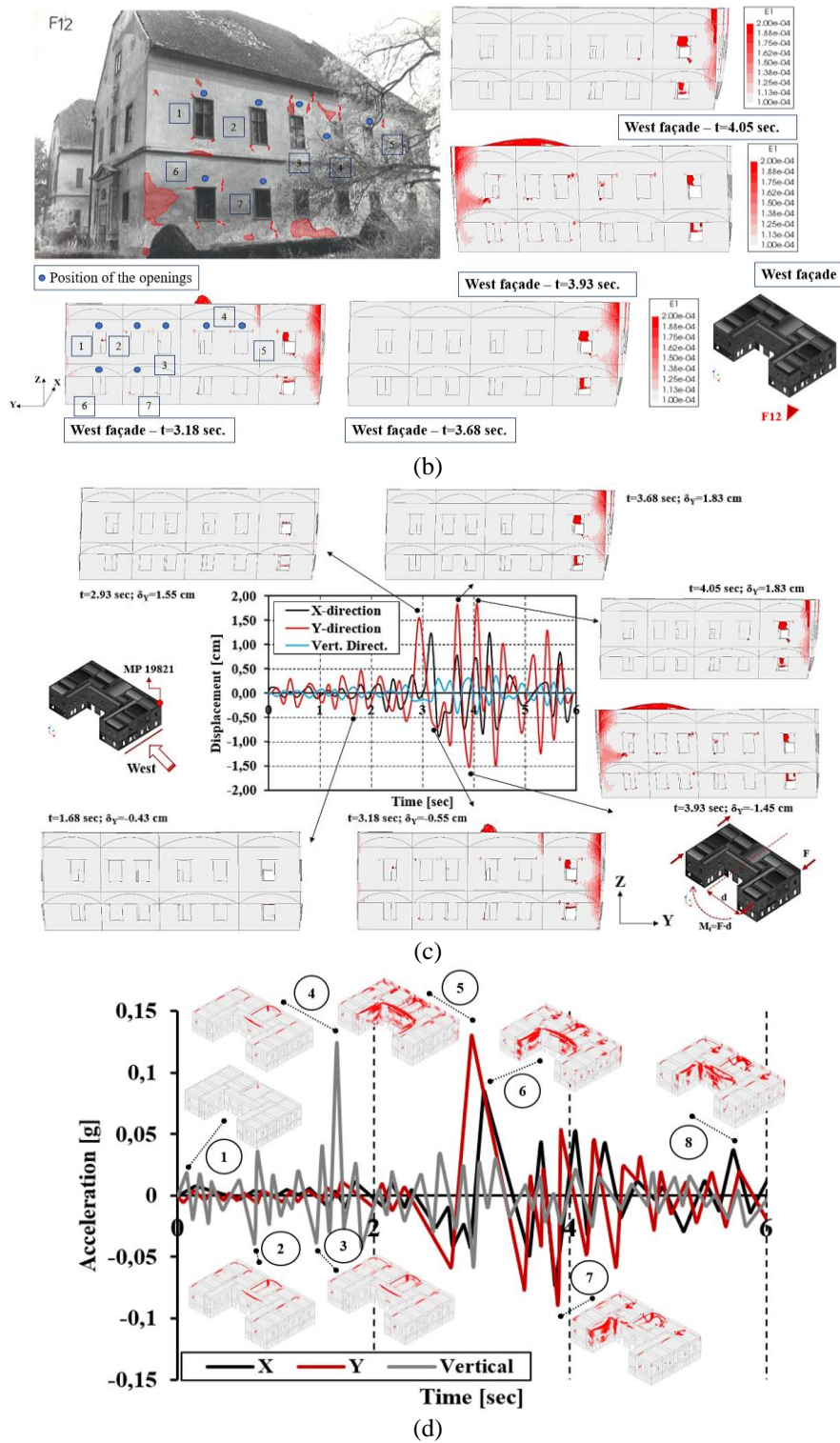


Figure 15: Numerical Vs real damage correlation.

It is noted how the numerical damage is not dissimilar from the damage that occurred in the epicentral area. It is worth underlining how the vertical component of the earthquake in the first two seconds of the time domain predominantly affects the horizontal structures. Subsequently, with the arrival of the horizontal seismic actions, the damage tends to spread to the vertical structures. This circumstance can be deduced from the fact that the high-frequency content of the vertical component cyclically degrades the axial and shear strength of the

masonry, favoring the formation of cracks [47].

Chapter five provides an accurate treatment for the derivation of fragility and vulnerability curves based on the numerical simulations performed. The first part of the chapter resumes the evaluation of the fragility curves in the case of a near-field earthquake. In the specific case, the fragility curves were derived considering the comparison between the two scenarios analysed, (H) and (H+V), respectively. In particular, it was possible to compare the effects induced by the ground motion vertical component on the global fragility assessment of the case study structure. It is also important to underline two fundamental aspects: (i) the simulated seismic phenomenon is impulsive and in the time domain the ground motion vertical component tends to maximize the effects at 1.68 sec; (ii) with the arrival of the horizontal components at $t > 2$ sec, the vertical seismic input progressively attenuates. To fully understand the effects induced by the ground motion vertical, the capacity curves at 33%, 50%, and 100% of the capacity of the structure have been considered.

First of all, according to [48], the fragility curves were defined in terms of displacement, S_d . This choice is supported by the fact that, in the case of impulsive seismic phenomena, the seismic response of the structure was analysed in terms of displacements which provided a quick and clear identification of the influence of the vertical component of seismic action on the global behavior of the considered study building. The results have been plotted in Fig. 16

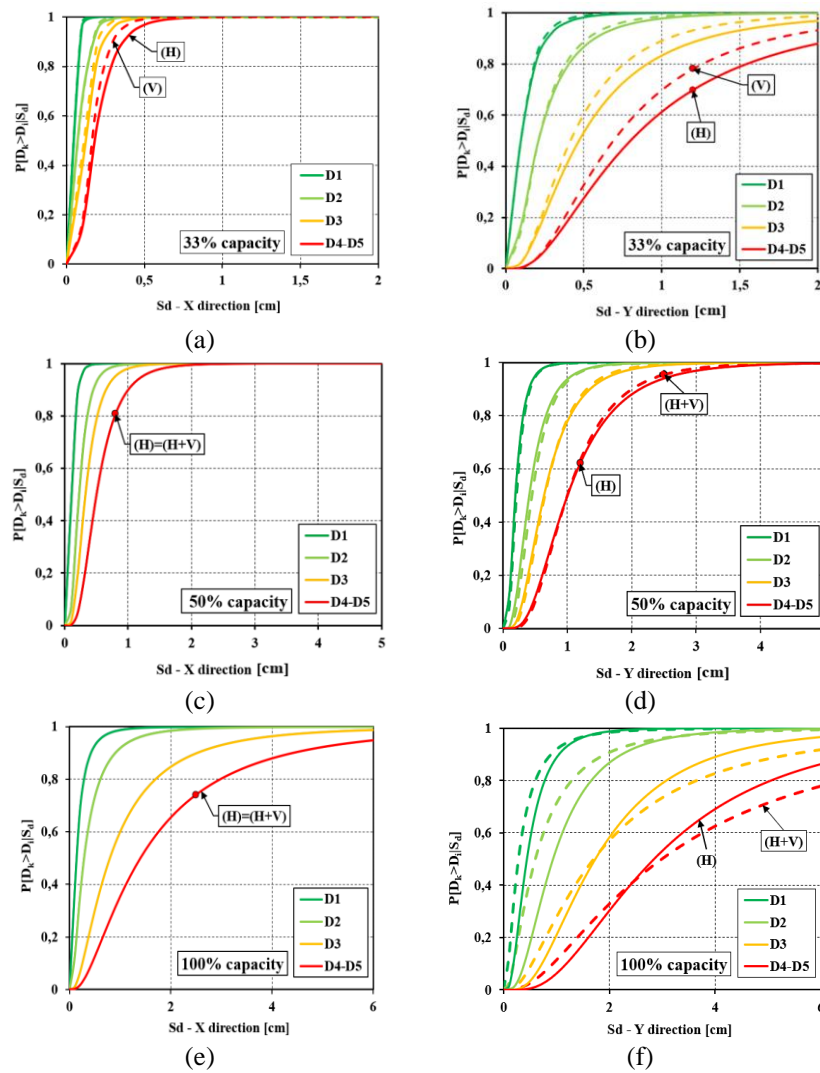


Figure 16: Fragility curves developed for (H) - (solid line) and (V) - (dashed line) scenario for a different level of structural capacity.

Referring to the condition of 33% of the structural capacity, it was noted that in both analysis directions, X and Y, the scenario (V) provides damage probabilities, associated with the damage thresholds D1 and D2, very close to the scenario (H). Furthermore, for a damage level D3 and D4-D5, it was noted that scenario (V) has provided a probability of occurrence of a specific damage threshold higher i.e. 13% than the scenario in which the vertical component of the seismic action was neglected, (H), resulting more vulnerable.

On the contrary, by analysing the behavior for a structural capacity equal to 100%, a significant increase of the spectral displacements has been noted compared to the cases examined previously. In this condition, the time history domain was completed and all the cumulative effects induced by vertical and horizontal seismic actions have been dissipated. It was noted as in X direction both scenarios analysed, (H) and (H+V), have provided the same probability in terms of damage thresholds D1-D5.

Nevertheless, in Y direction, it was noted that for damage thresholds D1 and D2, the scenario (H+V) provided a slightly higher probability of damage than the corresponding (H) since in the elastic field, the vertical component influence the displacements of the scenario (H+V) in which reached the exceeding of the elastic damage states first. Moreover, for damage thresholds D3 and D4-D5, the vertical component produced an improvement in terms of mechanical characteristics since the compressive vertical acceleration peak, despite their high-frequency content, has guaranteed an enhancement of the resistance while the decompressions peaks did not generate any type of localized structural deficit since they were properly balanced by gravitational loads.

In the second part of the chapter, the vulnerability curves have been derived, proposing a simplified formulation concerning the evaluation of the mean damage grade. The procedure proposed by [49] is not always applicable to every structural system, since it tends to underestimate the expected damage because it is calibrated on a set of buildings that are typologically and structurally different from what is generally found. The studies proposed by [50-52], have proposed some modifications to the formulation originally proposed by [49] for the evaluation of the mean damage grade. It was observed that the post-earthquake damage found in the scenario analyses obtained by using the mechanical approach was not correlated to the damage value achieved using the original formulation.

In particular, it was observed that for a shallow earthquake of a moment magnitude, $M_w=5.5$, the seismic intensity was equal to VII-VIII which corresponds to damage equal to D3-D4 (many buildings have serious cracks localized in the load-bearing walls). So, based on this consideration a vulnerability curves have been derived according to the original formula proposed by [53] considering both scenario (H) and (H+V) performed using both, non-linear static (NLSA) and dynamic analysis (TH) for the two-analysis direction, X and Y, having assumed a ductility factor Q equal to 2.3 [53]. The results have been reported in Fig. 17.

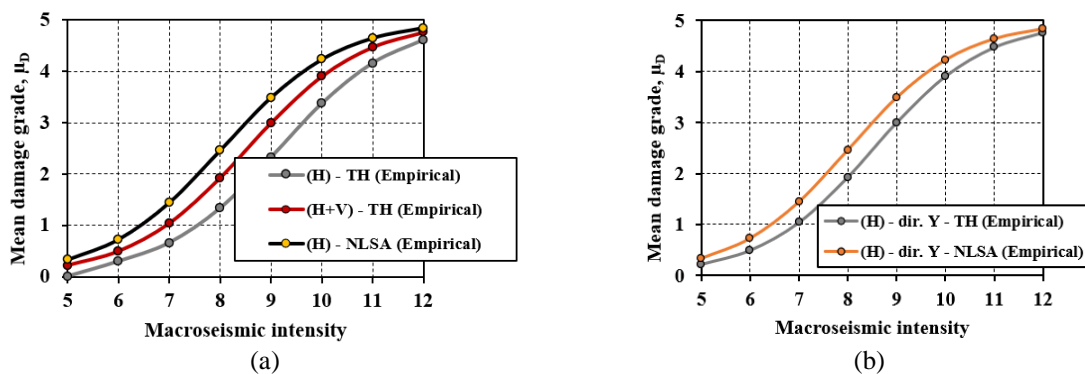


Figure 17: Vulnerability curves resumed through the empirical formulation [53].

The formulation proposed by [53] did not fully capture the level of damage that occurred for macroseismic intensity equal to VII-VIII, underestimating the real damage detected after the seismic event in 1991. Thus, is necessary to guarantee a mathematical formulation that correlates the observed damage that occurred in the epicenter, equal to D3-D4, to the macroseismic intensity of VII-VIII according to the EMS-98 scale [24].

The new formulation proposes: (i) a new corrective factor relative to the concavity of the curve assumed to be equal to 14.00; (ii) a correction factor that takes into account the variation in the slope of the curve assumed to be equal to 12.10; (iii) was assumed as a behavior factor $Q = 1.5$, as previously estimated by time-history analysis. The results have been presented in Fig. 18.

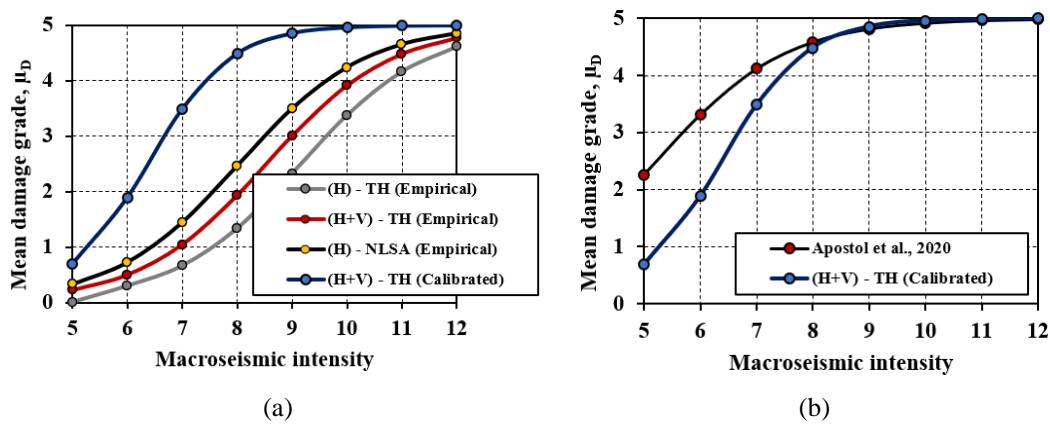


Figure 18: Calibrated typological vulnerability curves in the case of VGM (a) and empirical comparison with the formulation proposed by [54].

The proposed formulation, if compared with the method proposed by [54] provides safe and appreciable results in predicting the possible expected damage in the case of a near-field event. In general, the methodology proposed in this thesis could be further used for the evaluation of the seismic vulnerability of other historic masonry buildings characterized by the same typological and structural peculiarities located in the epicentral area. The seismic vertical component especially for shallow earthquakes is undoubtedly a high-risk factor to be taken into account in the analysis of seismic damage since it would guarantee a profitable forecasting activity for the protection of structures and mitigate possible disastrous effects.

Chapter six represents the conclusion of the entire thesis. The presented Ph.D. thesis aims to continue with particular attention the research topic started years ago by late lamented Prof. Eng. V. Gioncu and Prof. Eng. F. M. Mazzolani as part of the Prohitech European Research Contract concerning the seismic behavior of buildings located in the epicentral area.

In particular, studies over the years have provided, for the entire scientific community, an important starting point related to the assessment of the seismic vulnerability of historic masonry buildings subject to the near-field earthquake, providing a comprehensive overview regarding phenomenological aspects correlated to the induced effects on engineering structures. These prerogatives have been the basis for developing a systematic procedure for assessing the seismic performance level of a load-bearing capacity structure located in the Banat Seismic Region, mainly conditioned by medium-high seismicity.

The proposed methodology for assessing seismic vulnerability has a primary objective of providing a comprehensive overview for the implementation of analytical procedures for estimating the effects induced by the ground motion vertical component on historical masonry structures. The proposed methodology provides an accurate treatment of the main vulnerability factors that can be "altered" in the case of a seismic vertical component. In this sense, it has been underlined the importance of conducting specific numerical analyses that take into account this phenomenology to reduce the expected risk, safeguard historical and cultural heritage and providing appropriate evaluation procedures for different technical purposes, i.e. researchers and professional activity.

Regarding the personal contributions within the thesis, it is noted:

- The proposed methodology can be used to evaluate the seismic response of other historic masonry buildings (with similar construction techniques of the buildings sample located in the Banat region) in Europe subjected to shallow earthquakes with a medium-high intensity;
- For the first time, indications were provided on the dynamic characterization of the simulated seismic event focusing on the frequency contribution and the V/H ratio in case of near-field conditions. The maximum amplification ratio, V/H, was estimated equal to 2.2 for short period, $T=0.2$ sec;
- The research has shown that the ductility demand estimated in the longitudinal direction is reduced by about 4 times compared to the other direction since torsional phenomena, triggered by the ground motion horizontal components, limit the global capacity of the structure;
- For the first time, the effects induced by the vertical seismic component were estimated on the behavior factor, the stiffness degradation, respectively;
- The thesis showed how the ground motion vertical component negatively affects the global behavior of the structure by increasing the expected vulnerability in the case of the maximum decompression phase estimated at 1.68 sec. Conversely, at the time step 3.00 sec, the horizontal seismic actions trigger the structural damage assisted by the maximum compression produced by the vertical component. However, the vertical seismic decompression component reduces the capacity of the structure;
- The failure hierarchy induced by the ground motion vertical component was estimated for the first time to identify the expected in-plane mechanisms;
- A simplified procedure has been proposed for the calculation of the possible out-of-plane mechanisms in the case of a vertical earthquake;
- For the first time, damage indices were estimated that take into account the influence of the ground motion vertical excitation on the failure hierarchy of wall panels;
- For the first time the analytical fragility and vulnerability curves have been calibrated based on the real damage observed after the Banloc earthquake in case of a near-field earthquake;

The published papers have been disseminated in 26 scientific papers and 5 participations in international conferences. Of these, 6 papers have been published in indexed scientific journals Web of Science and 9 in volumes of indexed conferences Web of Science. The 26 papers are cited in turn in 92 indexed papers Web of Science and 170 indexed papers Scopus.

In conclusion, the Ph.D. thesis presents valuable contributions in the field of seismic

vulnerability of historic masonry buildings, while opening up future research directions of great interest for the reduction of seismic risk in the Banat area.

BIBLIOGRAPHY

- [1] M. Indirli, L.A.S. Kouris, A. Formisano, R.P. Borg, F.M. Mazzolani, Seismic damage assessment of unreinforced masonry structures after the Abruzzo 2009 earthquake: The case study of the historical centers of L'Aquila and Castelvechio Subequo, *International Journal of Architectural Heritage*, 7, 536–578, 2013.
- [2] P.G. Asteris, M.P. Chronopoulos, C.Z. Chrysostomou, H. Varum, V. Plevris, N. Kyriakides, V. Silva, Seismic vulnerability assessment of historical masonry structural systems, *Engineering Structures*, 62-63, 118-134, 2014.
- [3] L.F. Ramos, P.B. Lourenço, Modeling and vulnerability of historical city centers in seismic areas: A case study in Lisbon, *Engineering Structures*, 26, 1295–1310, 2004.
- [4] P.B. Lourenço, J.A. Roque, Simplified indexes for the seismic vulnerability of ancient masonry buildings, *Construction and Building Materials*, 20, 200-208, 2006.
- [5] N. Chieffo, I. Onescu, A. Formisano, M. Marius, Empirical-mechanical Seismic Vulnerability Analysis Method for Masonry Buildings in Timișoara: Validation based on the 2009 Italian Earthquake, *The Open Civil Engineering Journal*, 314-333, 2020.
- [6] M. Mosoarca, V. Gioncu, Assessment and mitigation procedures for historical buildings situated in seismic areas, in: *Proceedings of the International Conference on Risk Management, Assessment and Mitigation, RIMA'10*, 27-32, 2010.
- [7] F. Clementi, V. Gazzani, M. Poiani, S. Lenci, Assessment of seismic behaviour of heritage masonry buildings using numerical modelling, *Journal of Building Engineering*, 8, 29–47, 2016.
- [8] Eurocode 8, European Standard EN 1998-3:2005: Design of structures for earthquake resistance - Part 3: Assessment and retrofitting of buildings, Comité Européen de Normalisation, Brussels, 2005.
- [9] P100-1/2013 Cod de proiectare seismică – Partea I–Prevederi de proiectare pentru clădiri, O.M.D.R.A.P. nr. 2.956/18.11.2019, Monitorul Oficial al României Nr./dată M.Of., p I, nr.928/18.11.2019.
- [10] DM 17/01/2018, Aggiornamento delle “Norme Tecniche per le Costruzioni” - NTC 2018, 1–198, 2018 (in Italian).
- [11] O.D. Cardona, M.G. Ordaz, L.E. Yamin, M.C. Marulanda, A.H. Barbat, Earthquake loss assessment for integrated disaster risk management, *Journal of Earthquake Engineering*, 12, 48–59, 2008.
- [12] R. V. Whitman, J.W. Reed, S.-T. Hong, Earthquake Damage Probability Matrices, *Proceedings of the Fifth World Conference on Earthquake Engineering*, Rome, Italy, 2, 2531–2540, 1974.
- [13] F. Braga, D. Liberatore, M. Dolce, Fast and reliable damage estimation for optimal relief operations, in: *International Symposium on Earthquake Relief in Less Industrialized Areas (Zurich)*, 145–151, 1984.
- [14] G. Di Pasquale, G. Orsini, R.W. Romeo, New developments in seismic risk assessment in Italy, *Bulletin of Earthquake Engineering*, 3, 101-128, 2005.
- [15] M. Dolce, A. Kappos, A. Masi, G. Penelis, M. Vona, Vulnerability assessment and earthquake damage scenarios of the building stock of Potenza (Southern Italy) using Italian and Greek methodologies, *Engineering Structures*, 28, 357–371, 2006.
- [16] D. Benedetti and V. Petrini, “On the seismic vulnerability of masonry buildings: an evaluation method (in Italian),” *L'Industria delle Costruzioni*, vol. 149, pp. 66–74, 1984.
- [17] V. Petrini, “Rischio Sismico Di Edifici Pubblici, Parte I: Aspetti Metodologici,” in *Proceedings of CNR-Gruppo Nazionale per la Difesa dai Terremoti*, 1993.
- [18] F. Sabetta, A. Goretti, and A. Lucantoni, “Empirical fragility curves from damage surveys and estimated strong ground motion,” in *11th European Conference on Earthquake Engineering*, 1998.
- [19] A. Formisano, R. Landolfo, F. Mazzolani, and G. Florio, “A quick methodology for seismic vulnerability assessment of historical masonry aggregates,” *COST Action C26: Urban Habitat Constructions under Catastrophic Events*, no. September, 2010.

- [20] A. Singhal, A.S. Kiremidjian, Method for Probabilistic Evaluation of Seismic Structural Damage, *Journal of Structural Engineering*, 122, 1459–1467, 2002.
- [21] P. Moroux et al., “The European Risk-UE project: an advanced approach to earthquake risk scenarios,” in 13th World Conference on Earthquake Engineering, no. 423, 2004.
- [22] P. Fajfar, Capacity spectrum method based on inelastic demand spectra, *Earthquake Engineering and Structural Dynamics*, 28, 979–993, 1999.
- [23] F. E. M. Agency, FEMA Mitigation Division. HAZUS-MH MR3: Multi-Hazard Loss Estimation Methodology: Technical Manual. Washington DC, 2003.
- [24] G. Grünthal, European Macroseismic Scale 1998 (EMS-98), *Cahiers du Centre Européen de Géodynamique et de Séismologie* 15, Centre Européen de Géodynamique et de Séismologie, Luxembourg, 99, 1998.
- [25] A. Bala, D. Toma-Danila, M. Radulian, Focal mechanisms in Romania: statistical features representative for earthquake-prone areas and spatial correlations with tectonic provinces, *Acta Geodaetica et Geophysica*, 54, 263–286, 2019.
- [26] E. Oros, Seismological DataBase for Banat Seismic Region (Romania)-Part 1: The Parametric Earthquake Catalogue, *Romanian Journal of Physics*, 53 955–964, 2008.
- [27] Castelul Banloc, Wikiwand, available at: wikiwand.com (accessed September 25, 2020).
- [28] Earthquake Selection WebGIS App (BIGSEES), available at: <https://infop.maps.arcgis.com> (accessed October 20, 2020).
- [29] IPROTIM, Expertiza cu principii de consolidare (In Romanian), 1990.
- [30] DIANA FEA, Diana User’s Manual, Release 10.2, 2017.
- [31] I.S. Borcia, I. Craifaleanu, E.N. Tanase, E.I. Praun, Example of use of the SM-ROM-GL DataBase, in: 1st National Conference on Earthquake Engineering and Seismology 1CNISS, Bucharest, Romania, 1, 165–172, 2014.
- [32] N. Newmark, W. Hall, *Earthquake Spectra and Design*, EERI Monographs, 103 pages, 1982.
- [33] F. Di Michele, C. Cantagallo, E. Spacone, Effects of the vertical seismic component on seismic performance of an unreinforced masonry structures, *Bulletin of Earthquake Engineering*, 18, 1635–1656, 2020.
- [34] P.P. Diotallevi, L. Landi, Response of RC structures subjected to horizontal and vertical ground motions, in: 8th US National Conference on Earthquake Engineering, 2006.
- [35] G. Rinaldin, M. Fasan, S. Noé, C. Amadio, The influence of earthquake vertical component on the seismic response of masonry structures, *Engineering Structures*, 185, 184–193, 2019.
- [36] M. Acito, M. Bocciarelli, C. Chesi, G. Milani, Collapse of the clock tower in Finale Emilia after the May 2012 Emilia Romagna earthquake sequence: Numerical insight, *Engineering Structures*, 72, 70–91, 2014.
- [37] N. Chieffo, A. Formisano, M. Mosoarca, P.B. Lourenço, Seismic vulnerability assessment of a Romanian historical masonry building under near-source earthquake, in: XI International Conference on Structural Dynamic, EUROODYN20, 23–26 November, Athens, Greece, 4957–4971, 2020.
- [38] J. Ben Gu, Y. Tao, R. Xin, Z. Yang, Q.X. Shi, Seismic Performance of Multistorey Masonry Structure with Openings Repaired with CFRP Grid, *Advances in Civil Engineering*, Article ID 4374876, 11, 2018.
- [39] D. Zonta, G. Zanardo, C. Modena, Experimental evaluation of the ductility of a reduced-scale reinforced masonry building, *Materials and Structures*, 34, 636–644, 2001.
- [40] M. Tomaževič, P. Weiss, Displacement capacity of masonry buildings as a basis for the assessment of behavior factor: An experimental study, *Bulletin of Earthquake Engineering*, 8, 1267–1294, 2010.
- [41] M. Tomaževič, V. Bosiljkov, P. Weiss, Structural Behavior Factor for Masonry Structures, in: Proceedings of 13th World Conference on Earthquake Engineering, Vancouver, B.C., Canada, Paper No. 2642, 2004.
- [42] V. Turnšek, F. Čačovič, Some experimental results on the strength of brick masonry walls, in: Proceedings of the 2nd International Brick Masonry Conference, 149–156, 1971.
- [43] N. Augenti, *Il calcolo sismico degli edifici in muratura*, 1st ed., Turin, Italy, 2004 (in Italian).
- [44] M. Mariani, F. Pugi, A. Francioso, Vertical component of the seismic action: amplified vulnerability of existing masonry buildings, in: Multibody Dynamics Conference ECCOMAS19, July 15–18, Duisburg, Germany, 3807–3835, 2019.

- [45] F. Comodini, G. Fagotti, M. Mezzi, V.R. Vecchia, Effects of the earthquake vertical component in masonry buildings: vertical collapse mechanisms?, in: Proceedings of the 17th International Brick/Block Masonry Conference (17thIB2MaC 2020), July 5-8, Kraków, Poland, 2020.
- [46] S.T.A data srl, 3Muri 10.9.0 - User Manual, (n.d.).
- [47] V. Gioncu, F.M. Mazzolani, Earthquake Engineering for Structural Design, Spon Press (imprint of the Taylor & Francis Group), 581 pages, 2011, ISBN 0-203-84889-6.
- [48] S. Lagomarsino, S. Cattari, PERPETUATE guidelines for seismic performance-based assessment of cultural heritage masonry structures, Bulletin of Earthquake Engineering, 13, 13–47, 2015.
- [49] S. Lagomarsino, S. Giovinazzi, Macroseismic and mechanical models for the vulnerability and damage assessment of current buildings, Bulletin of Earthquake Engineering, 4, 415–443, 2006.
- [50] N. Chieffo, A. Formisano, T. Miguel Ferreira, Damage scenario-based approach and retrofitting strategies for seismic risk mitigation: an application to the historical Centre of Sant’Antimo (Italy), European Journal of Environmental and Civil Engineering, 2019, doi:10.1080/19648189.2019.1596164.
- [51] N. Chieffo, F. Clementi, A. Formisano, S. Lenci, Comparative fragility methods for seismic assessment of masonry buildings located in Muccia (Italy), Journal of Building Engineering, 25, 100813, 2019.
- [52] M. Mosoarca, I. Onescu, E. Onescu, B. Azap, N. Chieffo, M. Szitar-Sirbu, Seismic vulnerability assessment for the historical areas of the Timisoara city, Romania, Engineering Failure Analysis, 101, 86–112, 2019.
- [53] S. Lagomarsino, On the vulnerability assessment of monumental buildings, Bulletin of Earthquake Engineering, 4, 445–463, 2006.
- [54] I. Apostol, Seismic vulnerability assessment of historical urban centres, PhD Thesis, Politehnica University of Timisoara, 2020.